Contribution from the Chemistry and Materials Science Divisions, Argonne National Laboratory, Argonne, Illinois 60439, Department of General & Organic Chemistry, University of Copenhagen, Copenhagen, Denmark, and Department of Chemistry, North Carolina State University, Raleigh, North Carolina 27650

Crystal Structures of $[Au(DDDT)_2]^0$ and $[(n\text{-}Bu)_4N][Ni(DDDT)_2]$ and the Ligandlike Character of the Isoelectronic Radicals $[Au(DDDT)_2]^0$ and $[Ni(DDDT)_2]^-$

Arthur J. Schultz,*† Hau H. Wang,† Lynda C. Soderholm,† Thomas L. Sifter,† Jack M. Williams,*† Klaus Bechgaard,‡ and Myung-Hwan Whangbo*§

Received May 19, 1987

Use of the dithiolene ligand 5,6-dihydro-1,4-dithiin-2,3-dithiolate (DDDT) led to the new gold complex $[Au(DDDT)_2]^0$. Our single-crystal X-ray diffraction study shows that the crystal of $[Au(DDDT)_2]^0$ molecules packs in a dimerlike motif as found for the crystal of neutral ET molecules. In terms of valence electrons, $[Au(DDDT)_2]^0$ and $[Ni(DDDT)_2]^-$ molecules are isoelectronic. The present molecular orbital calculations suggest that the metal ions of both molecules are best described as d^8 ions as expected for square-planar metal complexes, and so an unpaired electron in each molecule resides largely on the DDDT ligands with a small delocalization into the metal ion. The crystal of $[Au(DDDT)_2]^0$ molecules shows no ESR absorption, which is likely due to the dimerlike packing motif and can be regarded as a consequence of a strong spin-Peierls distortion. We also report the synthesis, single-crystal X-ray structure, and magnetic susceptibility of $[(n\text{-}Bu)_4N][Ni(DDDT)_2]$. In this salt, $[Ni(DDDT)_2]^-$ molecules are found to form stacks, in contrast to those in $[Et_4N][Ni(DDDT)_2]$, which form layers. Unit cell parameters for $[Au(DDDT)_2]^0$ are space group $P2_1/n$, a = 6.496 (1) Å, b = 13.267 (4) Å, c = 16.775 (3) Å, β = 94.87 (2)°, V = 1440.5 (5) Å^3, and Z = 4. For $[(n\text{-}Bu)_4N][Ni(DDDT)_2]$, the space group is $P\bar{1}$, a = 9.126 (6) Å, b = 13.519 (9) Å, c = 13.723 (5) Å, α = 86.31 (4)°, β = 89.59 (4)°, γ = 77.58 (5)°, V = 1650 (2) Å^3, and Z = 2.

Introduction

Bis(dithiolene) complexes of metals are possible candidates for counteranions in conducting molecular solids,[1-3] one of which is reported[1b] to be superconducting at 1.62 K under a hydrostatic pressure of 7 kbar. An appealing feature of 5,6-dihydro-1,4-dithiin-2,3-dithiolate (DDDT) is that its metal complex $[M(DDDT)_2]^n$ (**1**)[3] is similar in structure to bis(ethylenedithio)-tetrathiafulvalene (BEDT-TTF or ET; **2**), which recently led to

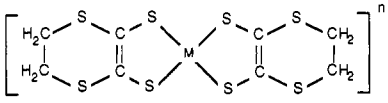

$[M(DDDT)_2]^n$

1

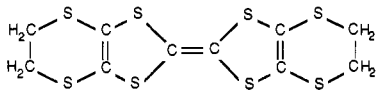

BEDT-TTF or ET

2

the ambient-pressure superconductors β-$(ET)_2X$ ($X^- = I_3^-$, AuI_2^-, IBr_2^-).[4] In the present work, we report the synthesis, structure, and physical properties of $[Au(DDDT)_2]^0$ and $[(n\text{-}Bu)_4N][Ni(DDDT)_2]$. In terms of valence electrons, $[Au(DDDT)_2]^0$ is isoelectronic with $[Ni(DDDT)_2]^-$ in $(Et_4N)[Ni(DDDT)_2]$[3] and in $[(n\text{-}Bu)_4N][Ni(DDDT)_2]$. The metal coordination geometry is square planar in both $[Au(DDDT)_2]^0$ and $[Ni(DDDT)_2]^-$, and they have one unpaired electron per molecule. To investigate whether the unpaired electron resides primarily on the metal ion or on the DDDT ligands, we also carry out molecular orbital (MO) calculations on $[Au(DDDT)_2]^0$ and $[Ni(DDDT)_2]^-$ based upon the extended Hückel method.[5]

Experimental Section

Synthesis of $[(n\text{-}Bu)_4N][Au(DDDT)_2]$ from $KAuBr_4$. The DDDT dianion was generated in situ under argon by treating TTBEO[6] (0.5 g, 2.4 mmol) with NaOEt (9.6 mmol) in absolute ethanol. After addition of the ligand solution to $KAuBr_4$ (0.65 g, 1.2 mmol) and filtration of the mixture in air, $[(n\text{-}Bu)_4N][Au(DDDT)_2]$ was precipitated with $[(n\text{-}Bu)_4N]Br$ (0.38 g, 1.2 mmol). Two recrystallizations from CH_2Cl_2/$(Et)_2O$ gave 0.56 g of analytically pure $[(n\text{-}Bu)_4N][Au(DDDT)_2]$ (60% yield), mp 206–207 °C.

Synthesis of $[(n\text{-}Bu)_4N][Au(DDDT)_2]$ from $[(n\text{-}Bu)_4N]AuCl_4$. A 0.01-mol amount of TTBEO[6] was treated with 0.02 mol of NaOMe in 25 mL of dry methanol until the solid had dissolved. To this solution was added 0.005 mol of $[(n\text{-}Bu)_4N]AuCl_4$ dissolved in 10 mL of dry methanol. After the mixture was stirred for 30 min, 100 mL of cold water was added to precipitate $[(n\text{-}Bu)_4N][Au(DDDT)_2]$. The product was filtered, dried, and purified by repeated reprecipitation from CH_2Cl_2 (63% yield, off-white needles).

Chemical Synthesis of $[Au(DDDT)_2]^0$. Treating $[(n\text{-}Bu)_4N][Au(DDDT)_2]$ with $[(n\text{-}Bu)_4N]I_3$ at room temperature in CH_2Cl_2 gave no apparent reaction. Reacting $[(n\text{-}Bu)_4N][Au(DDDT)_2]$ with $[(n\text{-}Bu)_4N]Br_3$ under the same conditions leads to immediate microcrystalline precipitation. By slow diffusion of dilute tribromide solution through a fine glass frit into a solution containing $[(n\text{-}Bu)_4N][Au(DDDT)_2]$, shiny black crystals of $[Au(DDDT)_2]^0$ were obtained.

Electrochemical Synthesis of $[Au(DDDT)_2]^0$. A 30-mg sample of $[(n\text{-}Bu)_4N][Au(DDDT)_2]$ was dissolved in 20 mL of a 0.1 M solution of $[(n\text{-}Bu_4N)]BF_4$ in methylene chloride. Electrochemical oxidation of $[(n\text{-}Bu)_4N][Au(DDDT)_2]$ was carried out with a 2-cm Pt rod (0.1 mm) as the anode and a constant current of 5 μA. Black needles of $[Au(DDDT)_2]^0$ were harvested after 5 days.

Synthesis of $[(n\text{-}Bu)_4N][Ni(DDDT)_2]$. The compound was prepared by following the same procedure as described above. The chemicals used are as follows: TTBEO[6] (1.07 g, 5.1 mmol), NaOEt (7.6 mL, 204 mmol), $NiCl_2 \cdot 6H_2O$ (0.61 g, 2.6 mmole), and $[(n\text{-}Bu)_4N]Br$ (0.86 g, 2.6 mmol). A total of 1.08 g of analytically pure $[(n\text{-}Bu)_4N][Ni(DDDT)_2]$ was obtained after recrystallization from $CH_2Cl_2/(Et)_2O$: mp 188 °C; 63% yield.

Single-Crystal X-ray Analyses. $[Au(DDDT)_2]^0$: space group $P2_1/n$, a = 6.496 (1) Å, b = 13.267 (4) Å, c = 16.775 (3) Å, β = 94.87 (2)°, V = 1440.5 (5) Å^3, Z = 4. X-ray intensity data were collected on a Nicolet P3/F diffractometer (ω scans, Mo Kα radiation, graphite monochromator, λ = 0.7107 Å) in the range $3° < 2\theta < 45°$ and were corrected for absorption (analytical, μ = 115.9 cm^{-1}). The structure was

† Argonne National Laboratory.
‡ University of Copenhagen.
§ North Carolina State University.

(1) (a) Bousseau, M.; Valade, L.; Legros, J.-P.; Cassoux, P.; Garbauskas, M.; Interrante, L. V. *J. Am. Chem. Soc.* **1986**, *100*, 1908. (b) Brossard, L.; Ribault, M.; Bousseau, M.; Valade, L.; Cassoux, P. *C. R. Acad. Sci., Ser. 2* **1986**, *302*, 205.
(2) Kobayashi, H.; Kato, R.; Kobayashi, A.; Sasaki, Y. *Chem. Lett* **1985**, 191.
(3) Vance, C. T.; Bereman, R. D.; Bordner, J.; Hatfield, W. E.; Helms, J. H. *Inorg. Chem.* **1985**, *24*, 2905.
(4) For a review, see: Williams, J. M.; Beno, M. A.; Wang, H. H.; Leung, P. C. W.; Emge, T. J.; Geiser, U.; Carlson, K. D. *Acc. Chem. Res.* **1985**, *18*, 261.
(5) Hoffmann, R. *J. Chem. Phys.* **1963**, *13*, 1397.
(6) Hartke, K.; Kissel, T.; Quante, J.; Matusch, R. *Chem. Ber.* **1980**, *113*, 1898. TTBEO is 2,5,7,9-tetrathiabicyclo[4.3.0]non-1(6)-en-8-one.

0020-1669/87/1326-3757$01.50/0

Table I. Atomic Positional and Thermal Parameters for $Au(DDDT)_2$[a]

atom	x	y	z	U_{iso}, Å^2
Au	−0.1104 (2)	0.0753 (1)	0.11804 (7)	0.0301 (4)
S(1)	0.076 (1)	0.0538 (8)	0.2381 ()	0.045 (4)
S(2)	−0.392 (1)	0.0016 (8)	0.1706 (5)	0.033 (3)
S(3)	−0.301 (2)	0.1018 (6)	−0.0025 (4)	0.039 (3)
S(4)	0.171 (1)	0.1492 (9)	0.0650 (5)	0.049 (4)
S(5)	0.024 (2)	−0.046 (1)	0.3872 (6)	0.068 (5)
S(6)	−0.472 (2)	−0.1021 (9)	0.3147 (6)	0.062 (5)
S(7)	−0.263 (2)	0.2351 (9)	−0.1374 (5)	0.050 (4)
S(8)	0.224 (1)	0.2823 (9)	−0.0686 (5)	0.044 (4)
C(1)	−0.096 (5)	−0.010 (3)	0.291 (2)	0.032 (9)*
C(2)	−0.289 (5)	−0.043 (2)	0.267 (2)	0.016 (7)*
C(3)	−0.140 (4)	0.174 (2)	−0.048 (1)	0.004 (6)*
C(4)	0.066 (5)	0.198 (3)	−0.020 (2)	0.031 (8)*
C(5)	−0.175 (6)	−0.123 (3)	0.436 (2)	0.040 (10)*
C(6)	−0.382 (6)	−0.088 (3)	0.418 (2)	0.058 (11)*
C(7)	−0.068 (5)	0.231 (3)	−0.206 (2)	0.026 (8)*
C(8)	0.115 (7)	0.268 (3)	−0.174 (2)	0.049 (10)*

[a] Values with an asterisk are for atoms refined isotropically. For atoms refined anisotropically, $U_{iso} = {}^1/_3\sum_i\sum_j U_{ij}a_i^*a_j^*\mathbf{a}_i\cdot\mathbf{a}_j$.

Table II. Atomic Positional and Thermal Parameters for $[(n\text{-Bu})_4][Ni(DDDT)_2]$[a]

atom	x	y	z	U_{iso}, Å^2
Ni(1)	0.0	0.0	0.0	0.065 (2)
Ni(2)	0.0	0.5	0.5	0.067 (2)
S(11)	0.1736 (6)	−0.1290 (4)	0.0399 (4)	0.087 (3)
S(12)	0.1383 (6)	0.0511 (4)	−0.1094 (4)	0.088 (3)
S(13)	0.4781 (7)	−0.2181 (5)	−0.0260 (4)	0.110 (3)
S(14)	0.4373 (7)	−0.0220 (5)	−0.1937 (5)	0.115 (4)
S(21)	−0.1798 (6)	0.4224 (4)	0.4863 (4)	0.088 (3)
S(22)	0.1059 (6)	0.4347 (5)	0.3728 (4)	0.090 (3)
S(23)	−0.2738 (8)	0.2880 (6)	0.3557 (5)	0.137 (4)
S(24)	0.0393 (8)	0.3062 (6)	0.2230 (5)	0.139 (4)
C(11)	0.320 (2)	−0.117 (2)	−0.042 (1)	0.072 (11)
C(12)	0.304 (2)	−0.041 (1)	−0.104 (1)	0.063 (10)
C(13)	0.624 (2)	−0.173 (2)	−0.105 (2)	0.149 (16)
C(14)	0.617 (3)	−0.083 (2)	−0.139 (2)	0.126 (15)
C(21)	−0.144 (2)	0.355 (2)	0.383 (1)	0.068 (11)
C(22)	−0.012 (3)	0.363 (1)	0.334 (2)	0.090 (12)
C(23)	−0.197 (4)	0.210 (2)	0.259 (2)	0.181 (23)
C(24)	−0.086 (4)	0.224 (3)	0.204 (2)	0.194 (24)
N	0.464 (2)	0.298 (1)	−0.313 (1)	0.086 (5)*
C(N11)	0.517 (2)	0.394 (2)	−0.301 (1)	0.098 (8)*
C(N12)	0.572 (2)	0.403 (2)	−0.192 (2)	0.109 (8)*
C(N13)	0.608 (3)	0.510 (2)	−0.181 (2)	0.144 (10)*
C(N14)	0.675 (3)	0.516 (2)	−0.094 (2)	0.129 (9)*
C(N21)	0.342 (2)	0.282 (1)	−0.244 (1)	0.071 (6)*
C(N22)	0.196 (2)	0.365 (2)	−0.260 (1)	0.096 (8)*
C(N23)	0.066 (2)	0.343 (1)	−0.191 (1)	0.098 (7)*
C(N24)	0.114 (3)	0.373 (2)	−0.089 (2)	0.137 (10)*
C(N31)	0.419 (2)	0.296 (2)	−0.425 (1)	0.081 (7)*
C(N32)	0.370 (3)	0.203 (2)	−0.447 (2)	0.121 (9)*
C(N33)	0.368 (3)	0.192 (2)	−0.556 (2)	0.170 (12)*
C(N34)	0.315 (3)	0.109 (2)	−0.579 (2)	0.155 (11)*
C(N41)	0.599 (2)	0.205 (1)	−0.291 (1)	0.074 (6)*
C(N42)	0.743 (2)	0.212 (2)	−0.349 (1)	0.097 (7)*
C(N43)	0.849 (2)	0.108 (2)	−0.329 (1)	0.096 (7)*
C(N44)	0.998 (2)	0.106 (2)	−0.391 (1)	0.121 (9)*

[a] Values with an asterisk are for atoms refined isotropically. For atoms refined anisotropically, $U_{iso} = {}^1/_3\sum_i\sum_j U_{ij}a_i^*a_j^*\mathbf{a}_i\cdot\mathbf{a}_j$.

solved from a Patterson synthesis map. Full-matrix least-squares refinement (114 variables, anisotropic thermal parameters for gold and sulfur atoms, isotropic thermal parameters for carbon atoms, anomalous scattering included) yielded $R(F) = 0.088$, $R_w(F) = 0.059$, and GOF = 1.35 for 1150 reflections with $|F| > 3\sigma(|F|)$.

$[(n\text{-Bu})_4N][Ni(DDDT)_2]$: space group $P\bar{1}$, $a = 9.126$ (6) Å, $b = 13.519$ (9) Å, $c = 13.723$ (5) Å, $\alpha = 86.31$ (4)°, $\beta = 89.59$ (4)°, $\gamma = 77.58$ (5)°, $V = 1650$ (2) Å^3, $Z = 2$. X-ray intensity data were collected on a Krisel automated Picker diffractometer (θ–2θ scans, Mo Kα radiation, graphite momochromator, $\lambda = 0.7107$ Å) in the range $3° < 2\theta < 40°$ and were corrected for absorption (analytical, $\mu = 10.92$ cm^{-1}). The structure was solved by direct methods. Full-matrix least-squares refinements (225 variables, anisotropic thermal parameters for $[Ni(DDDT)_2]^-$ atoms, isotropic thermal parameters for $[(n\text{-Bu})_4N]^+$ atoms, anomalous scattering included) yielded $R(F) = 0.095$, $R_w(F) = 0.072$, and GOF = 1.62 for 1528 reflections with $|F| > 3\sigma(|F|)$.

Table III. Cyclic Voltammetry Data for $[Au(DDDT)_2]^n$

oxidn $n \rightarrow n+1$	$E_{1/2}$, V[a]
$-2 \rightarrow -1$	−1.32[b]
$-1 \rightarrow 0$	+0.41
$0 \rightarrow +1$	(+0.82)[c]

[a] The scan rate was 0.2 V/s, and voltages are relative to SCE. [b] Jenkins, J. J., II. *Diss. Abstr. Int.*, *B* **1978**, *38*, 5364. [c] Quasi-reversible.

Table IV. Intramolecular Distances and Angles in $Au(DDDT)_2$

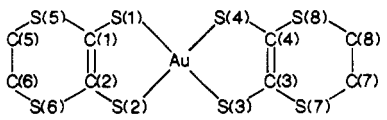

(a) Distances (Å)

Au–S(1)	2.280 (9)	S(6)–C(2)	1.69 (3)
Au–S(2)	2.312 (9)	S(6)–C(6)	1.78 (4)
Au–S(3)	2.306 (8)	S(7)–C(3)	1.84 (3)
Au–S(4)	2.317 (9)	S(7)–C(7)	1.78 (3)
S(1)–C(1)	1.71 (3)	S(8)–C(4)	1.76 (3)
S(2)–C(2)	1.80 (3)	S(8)–C(8)	1.87 (4)
S(3)–C(3)	1.65 (3)	C(1)–C(2)	1.35 (4)
S(4)–C(4)	1.66 (3)	C(3)–C(4)	1.42 (4)
S(5)–C(1)	1.80 (3)	C(5)–C(6)	1.43 (5)
S(5)–C(5)	1.89 (4)	C(7)–C(8)	1.35 (5)

(b) Angles (deg) around Gold Atom

S(1)–Au–S(2)	89.4 (3)	S(2)–Au–S(3)	90.9 (3)
S(1)–Au–S(3)	178.4 (4)	S(2)–Au–S(4)	179.8 (3)
S(1)–Au–S(4)	90.8 (3)	S(3)–Au–S(4)	88.9 (3)

The atomic positional coordinates for $[Au(DDDT)_2]^0$ and $[(n\text{-Bu})_4N][Ni(DDDT)_2]$ are listed in Tables I and II, respectively. Anisotropic thermal parameters and observed and calculated structure factors for $[Au(DDDT)_2]^0$ and $[(n\text{-Bu})_4N][Ni(DDDT)_2]$ are given in the supplementary material.

Cyclic Voltammetry (CV) Measurements. The CV data for $[Au(DDDT)_2]^n$ ($n = 0, -1, -2$) were measured in a CH_2Cl_2 solution containing 0.2 M $[(n\text{-Bu})_4N]PF_6$ and with a Pt-button electrode, which are summarized in Table III. Both $[Au(DDDT)_2]^{2-}$ and $[Au(DDDT)_2]^-$ are reversibly oxidized. The oxidation to $[Au(DDDT)_2]^0$ occurs at a moderately positive potential. The stability of the neutral species $[Au(DDDT)_2]^0$ may be related to the fact that the oxidized ligand, tetrathiooxalic acid ethylene ester, is chemically stable.[6]

Magnetic Susceptibility Measurements on $[(n\text{-Bu})_4N][Ni(DDDT)_2]$. Magnetic susceptibility data were obtained with a George Associates Lewis Coil force magnetometer. Fields were varied to 6000 Oe, measured with a precalibrated Hall probe. Temperatures over the range $4 < T < 300$ K were monitored by a Ni–Cr vs Cu–Ni (chromel–constantan) thermocouple.

Results and Discussion

A. Crystal Structures. $[Au(DDDT)_2]^0$. Two different synthetic routes to $[Au(DDDT)_2]^0$, described above, produce shiny black needlelike crystals of $[Au(DDDT)_2]^0$. Table IV contains selected intramolecular bond distances and angles. The bond lengths are apparently asymmetric, which is probably unreal since they have large standard deviations. In an attempt to improve the structural results, we collected a second data set at 125 K, but the results were even less satisfactory than those of the room-temperature structure. At the present moment we do not know the cause for this problem, but it is clear that the molecular conformation of $[Au(DDDT)_2]^0$ and the packing of these molecules in solids is essentially correct.

Shown in Figure 1a is a projection view of the unit cell on the *bc* plane, which indicates that the $[Au(DDDT)_2]^0$ molecules pack as "dimers" with the crystallographic inversion centers at (0, 0, 0) and $(a/2, b/2, c/2)$. This packing motif is virtually identical with that found for the crystal of neutral ET molecules,[7] shown

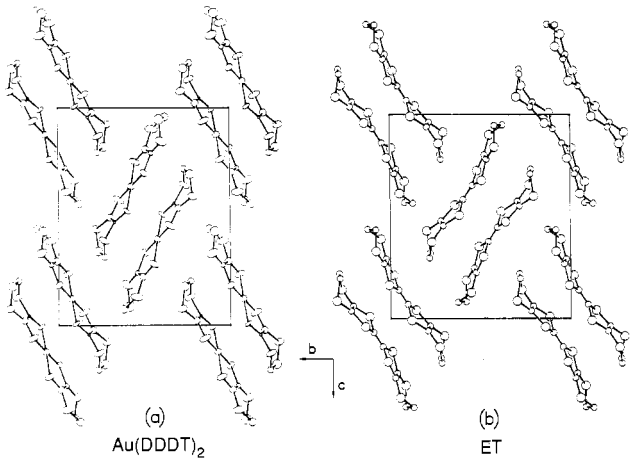

Figure 1. (a) Projection on the *bc* plane of the crystal structure of $Au(DDDT)_2$. The molecules form nonbonding dimeric pairs about crystallographic inversion centers. The dimer in the center is above the plane of the other molecules by $a/2$. Thermal ellipsoids are drawn at the 50% probability level. (b) The same projection for the crystal structure of neutral ET (adapted from ref 7).

Table V. Intramolecular Distances and Angles in $[(n\text{-}Bu)_4][Ni(DDDT)_2]$

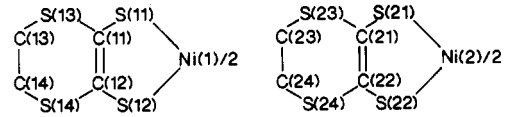

(a) Distances (Å) in $[Ni(DDDT)_2]^-$ Anions

Ni(1)–S(11)	2.134 (12)	Ni(2)–S(21)	2.145 (9)
Ni(1)–S(12)	2.130 (6)	Ni(2)–S(22)	2.137 (6)
S(11)–C(11)	1.76 (2)	S(21)–C(21)	1.73 (2)
S(12)–C(12)	1.74 (2)	S(22)–C(22)	1.70 (2)
S(13)–C(11)	1.76 (2)	S(23)–C(21)	1.69 (2)
S(13)–C(13)	1.89 (2)	S(23)–C(23)	1.79 (3)
S(14)–C(12)	1.77 (2)	S(24)–C(22)	1.77 (2)
S(14)–C(14)	1.81 (2)	S(24)–C(24)	1.79 (3)
C(11)–C(12)	1.28 (2)	C(21)–C(22)	1.40 (2)
C(13)–C(14)	1.27 (3)	C(23)–C(24)	1.29 (3)

(b) Angles (deg) around Nickel Atoms

S(11)–Ni(1)–S(12)	91.1 (2)	S(21)–Ni(2)–S(22)	91.1 (2)
S(11)–Ni(1)–S(12)′	88.9 (2)	S(21)–Ni(2)–S(22)′	88.9 (2)

in Figure 1b. As depicted in Figure 2, $[Au(DDDT)_2]^0$ molecules are cross-linked in three dimensions by intermolecular S···S contacts approximately equal to the van der Waals radii sum (3.60 Å). The gold coordination geometry is square planar, with the four cis S–Au–S angles varying from 88.9 (3) to 90.9 (3)° and the average Au–S distance of 2.30 (2) Å. These structural features compare well with those determined for $[Au(S_2C_2(CF_3)_2)_2]^-$.[8]

$[(n\text{-}Bu)_4N][Ni(DDDT)_2]$. Table V lists selected intramolecular bond distances and angles for the two $[Ni(DDDT)_2]^-$ anions on two different inversion centers in the crystal. The large standard deviations and some anomalous values for S–C and C–C distances derived from the data are apparently due to large thermal amplitudes of vibration for both cation and anion atoms and possible conformational disorder. However, the molecular structure of the $[Ni(DDDT)_2]^-$ anions in $[(n\text{-}Bu)_4N][Ni(DDDT)_2]$ is essentially the same as that found for $(Et_4N)[Ni(DDDT)_2]$.[3] The stereo diagram of Figure 3 shows how $[Ni(DDDT)_2]^-$ and $[(n\text{-}Bu)_4N]^+$ species are packed in $[(n\text{-}Bu)_4N][Ni(DDDT)_2]$. There are two different kinds of $[Ni(DDDT)_2]^-$ molecules: those that form segregated stacks aligned approximately along the *a* axis, as shown in Figure 4, and those oriented roughly perpendicular to the stacks. The latter $[Ni(DDDT)_2]^-$ molecules are well-separated from one another, in contrast to those in the stacks. It is noted that, in $(Et_4N)[Ni(DDDT)_2]$, $[Ni(DDDT)_2]^-$ molecules do not form stacks but layers as shown in Figure 5. That is, the length and shape of the alkyl group in a tetraalkylammonium ion have an important consequence upon the nature of interaction between $[Ni(DDDT)_2]^-$ molecules. This is due probably to the requirement of close packing of $[Ni(DDDT)_2]^-$ molecules around each tetraalkylammonium ion.

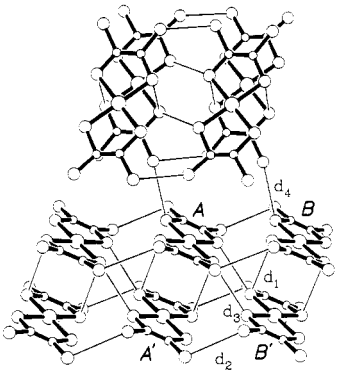

Figure 2. Perspective view of $[Au(DDDT)_2]^0$ in which the *b*+*c* diagonal is approximately vertical and the *a* axis is horizontal. For clarity, terminal ethylene groups have not been included. Intermolecular S···S distances approximately equal to or less than the van der Waals radii sum (3.60 Å) are shown as thin lines. Their values are d_1 = 3.61 (1) Å, d_2 = 3.59 (1) Å, d_3 = 3.66 (2) Å, and d_4 = 3.59 (1) Å.

Table VI. S···S Contacts

(a) ET (≤3.70 Å)[a]			
S(1)···S(2)′	3.69	S(5)···S(6)	3.69
S(1)···S(3)′	3.62	S(7)···S(8)′	3.55
S(4)···S(7)′	3.48		
(b) $Au(DDDT)_2$ (≤3.70 Å)			
S(1)···S(7)′	3.59 (1)	S(5)···S(6)′	3.66 (2)
S(2)···S(3)′	3.59 (1)	S(7)···S(8)′	3.67 (1)
S(3)···S(4)′	3.61 (1)		
(c) $[Et_4N][Ni(DDDT)_2]$ (≤4.25 Å)[b]			
S(1)···S(4)′	4.25	S(4)···S(4)′	4.25
S(3)···S(4)′	3.98		
(d) $[(n\text{-}Bu)_4N][Ni(DDDT)_2]$ (≤5.00 Å)			
S(11)···S(14)′	5.00 (2)	S(13)···S(14)′	4.75 (1)
S(12)···S(13)′	4.98 (2)		

[a] Reference 7. [b] Reference 3.

Table VI lists short intermolecular S···S contact distances found in the solids of neutral ET, $[Au(DDDT)_2]^0$, $(Et_4N)[Ni(DDDT)_2]$, and $[(n\text{-}Bu)_4N][Ni(DDDT)_2]^-$. It is inferred from Table VI that molecules are somewhat more tightly packed in ET than in $[Au(DDDT)_2]^0$ and adjacent $[Ni(DDDT)_2]^-$ molecules interact more strongly in $(Et_4N)[Ni(DDDT)_2]$ than in $[(n\text{-}Bu)_4N][Ni(DDDT)_2]$.

B. Electronic Structures and Physical Properties of $[M(DDDT)_2]^n$ Complexes (M = Ni, n = −1; M = Au, n = 0). The formal oxidation state of $[Au(DDDT)_2]^0$ may be written as $[Au^{4+}(d^7)](DDDT^{2-})_2$ or $[Au^{3+}(d^8)][(DDDT)_2^{3-}]$. Likewise, the formal oxidation state of $[Ni(DDDT)_2]^-$ can be written as $[Ni^{3+}(d^7)](DDDT^{2-})_2$ or $[Ni^{2+}(d^8)][(DDDT)_2^{3-}]$. For both complexes, the oxidation formalisms leading to d^7 and d^8 ions (hereafter referred to as the d^7 and d^8 oxidation formalisms, respectively) imply that one unpaired electron resides primarily on the metal ion and on the DDDT ligands, respectively. The fact that the metal coordination geometry of $[Au(DDDT)_2]^0$ and $[Ni(DDDT)_2]^-$ is square planar is more consistent with the d^8 oxidation formalism.

According to our MO calculations[9] on $[Ni(DDDT)_2]^-$, the

(7) Kobayashi, H.; Kobayashi, A.; Sasaki, Y.; Saito, G.; Inokuchi, H. *Bull. Chem. Soc. Jpn.* **1986**, *59*, 301. Unit cell parameters transformed into space group $P2_1/n$ are a = 6.614 Å, b = 13.985 Å, c = 15.721 Å, β = 93.81°, and V = 1451 Å^3.

(8) Enemark, J. H.; Ibers, J. A. *Inorg. Chem.* **1968**, *7*, 2636.

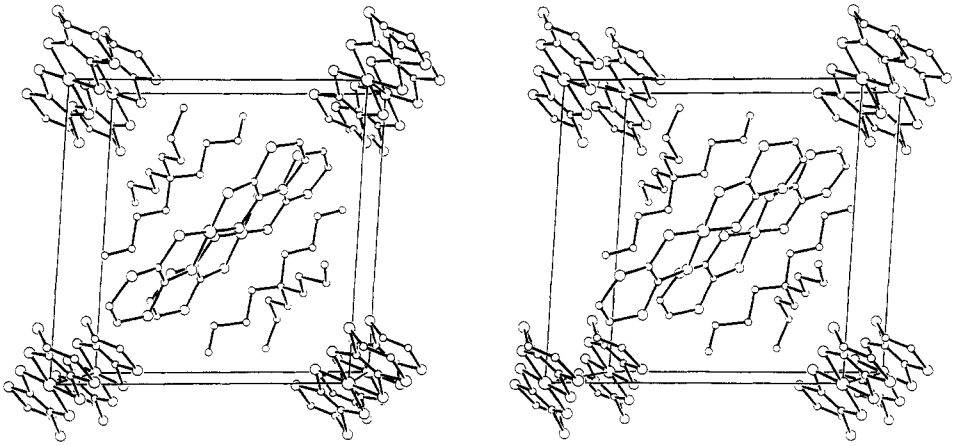

Figure 3. Stereoview of the unit cell of $[(n\text{-Bu})_4N][Ni(DDDT)_2]$. The view is approximately looking down the *a* axis, with *b* horizontal and *c* vertical on the paper.

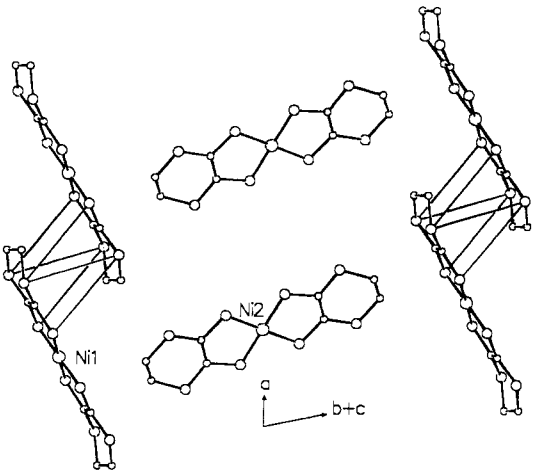

Figure 4. View along the "stacking" direction in $[(n\text{-Bu})_4N][Ni(DDDT)_2]$. Intermolecular interstack S···S contacts of 4.75–5.00 Å are shown as thin lines.

highest two filled MO's are mainly represented by the π^* orbitals of DDDT ligands as shown in **3a** and **3b**. The HOMO ψ_- is singly occupied and has a metal orbital character of less than 15%. Four MO's that can be classified as the metal d-block orbitals lie at least 1 eV below ψ_+. For instance, the d_{yz} MO shown in **4** lies ~1.3 eV below ψ_+. As a result, our calculations on $[Ni(DDDT)_2]^-$ are consistent with the d^8 oxidation formalism. The same is the case with our MO calculations on $[Au(DDDT)_2]^0$, whose highest two occupied MO's are again well-represented by the ligand orbitals ψ_+ and ψ_- shown in **3**.

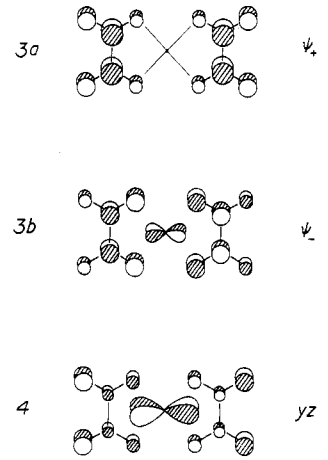

The magnetic susceptibility of $(Et_4N)[Ni(DDDT)_2]$ at high temperature leads to the magnetic moment of 1.9 μ_B, slightly greater than the spin-only moment of 1.73 μ_B expected for a system with one unpaired electron.[3] This result was employed[3] to support the d^7 oxidation formalism for $[Ni(DDDT)_2]^-$ but would be also consistent with the d^8 oxidation formalism if the single electron residing largely on the DDDT ligands is partially delocalized into the metal ion. In fact, the ESR data[3] on $[Ni(DDDT)_2]^-$ show a highly delocalized nature of the ground state. Furthermore, a long-range magnetic ordering is observed[3] in $(Et_4N)[Ni(DDDT)_2]$ despite the fact that the shortest intermolecular Ni···Ni distance is quite long (8.152 Å). This observation is easily accounted for, if the unpaired electron of $[Ni(DDDT)_2]^-$ resides primarily on the DDDT ligands as suggested by our MO calculations. The $[Ni(DDDT)_2]^-$ molecules in $(Et_4N)[Ni(DDDT)_2]$[3] are linked by intermolecular S···S contacts less than 4 Å to form a layered structure, as shown in Figure 5.

A plot of the inverse susceptibility vs temperature for $[(n\text{-Bu})_4N][Ni(DDDT)_2]$ is shown in Figure 6. Diamagnetic corrections have been made to the data by using the appropriate Pascal constants. The susceptibility is positive and varies smoothly from 4.2 K to room temperature, indicating that the tetra-*n*-butylammonium salt is paramagnetic over the temperature range studied. The magnitude of the susceptibility is consistent with one unpaired electron, as predicted by the calculations presented here. These results may be contrasted with those reported for the $(Et_4)N^+$ salt,[3] which exhibits long-range antiferromagnetic order below 15 K. Thus, it appears that, with the larger tetrabutylammonium cation, the $[Ni(DDDT)_2]^-$anions are further apart in the crystal, the S···S contacts are longer (see Table VI), and long-range magnetic coupling does not occur.

In our study, no ESR absorption was observed for $[Au(DDDT)_2]^0$, although one unpaired electron is formally present on each $[Au(DDDT)_2]^0$ molecule. It is likely, therefore, that the interaction between the $[Au(DDDT)_2]^0$ molecules in each "dimer" unit produces a diamagnetic spin-Peierls insulating state.[10] When a "dimer" of $[Au(DDDT)_2]^0$ is viewed normal to the molecular

(9) The atomic orbitals employed in our calculations are as follows: valence shell ionization potential H_{ii} (eV) and the exponent ζ_i of the Slater-type atomic orbital χ_i are respectively −20.0 and 2.122 for S 3s, −11.0 and 1.827 for S 3p, −21.4 and 1.625 for C 2s, −11.4 and 1.625 for C 2p, −13.6 and 1.3 for H 1s, −9.17 and 1.825 for Ni 4s, −6.86 and 1.85 for Ni 4p, −10.92 and 2.602 for Au 6s, and −5.55 and 2.584 for Au 6p. The d orbitals of Ni and Au are represented by a linear combination of two Slater-type orbitals of exponents ζ_i and ζ_i with weighting factors c_i and $\bar{c}_i$, respectively. The H_{ii} (eV), ζ_i, c_i, ζ_i, and $\bar{c}_i$ values are respectively −15.07, 6.163, 0.6851, 2.794, and 0.5696 for Au 5d and −13.49, 5.75, 0.5683, 2.00, and 0.6292 for Ni 3d. The off-diagonal Hamiltonian matrix elements H_{ij} were obtained by a modified Wolfsberg–Helmholz formula.[11]

(10) (a) Jacobs, S.; Bray, J. W.; Hart, H. R., Jr.; Interrante, L. V.; Kasper, J. S.; Watskin, G. D.; Prober, D. E.; Bonner, J. S. *Phys. Rev. B: Solid State* **1976**, *14*, 3036. (b) Bray, J. W.; Interrante, L. V.; Jacobs, I. S.; Bonner, J. C. In *Extended Linear Chain Compounds*; Miller, J. S., Ed.; Plenum: New York, 1983; Vol. 3, p 353.

(11) Ammeter, J. H.; Bürgi, H.-B.; Thibeault, J. C.; Hoffmann, R. *J. Am. Chem. Soc.* **1978**, *100*, 3686.

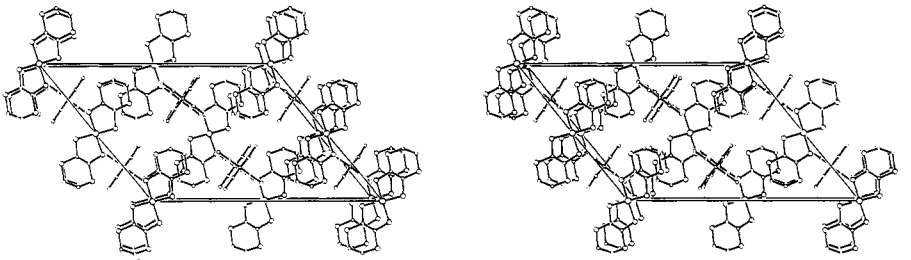

Figure 5. Stereoview of the unit cell of [Et$_4$N][Ni(DDDT)$_2$] (adapted from ref 3).

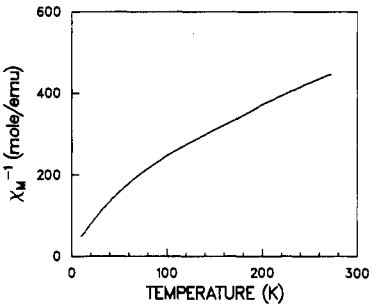

Figure 6. Plot of inverse magnetic susceptibility vs temperature for [(n-Bu)$_4$N][Ni(DDDT)$_2$].

plane, a gold atom of one [Au(DDDT)$_2$]^0 lies directly above the center of one of the two C=C bonds of the other [Au(DDDT)$_2$]^0. From the standpoint of covalent bonding, the interaction between the [Au(DDDT)$_2$]^0 molecules in each "dimer" cannot be strong because the closest intermolecular contact distances involving Au are long [i.e., Au···S3 = 4.16 (1) Å, Au···S4 = 4.27 (1) Å, and Au···Au = 4.765 (3) Å]. Nevertheless, the magnetic interaction between unpaired electrons within each "dimer" should be much stronger than the corresponding interaction between nearest-neighbor "dimers" in [Au(DDDT)$_2$]^0, because only such a situation will make the magnetic ground state well-separated from the magnetic excited state,[10] thereby suppressing an ESR absorption. The relative magnitudes of the interactions between nearest-neighbor unpaired electrons in [Au(DDDT)$_2$]^0 can be estimated in terms of the HOMO interaction integrals defined as

$$\beta_{ij} = \langle \psi_i | H^{eff} | \psi_j \rangle \quad (1)$$

where ψ_i and ψ_j are the HOMO's of the nearest-neighbor [Au(DDDT)$_2$]^0 molecules i and j in the crystal (e.g. i, j = A, A′, B, and B′ in Figure 2). For a pair of antiferromagnetically interacting electrons located on the molecules i and j, the magnetic exchange parameter J_{ij} is approximately related to β_{ij} as

$$J_{ij} \propto \beta_{ij}/U \quad (2)$$

where U is the so-called on-site Coulomb repulsion.[10] The β_{ij} values calculated for [Au(DDDT)$_2$]^0 are 0.20, 0.06, and 0.04 eV for the pairs (i,j) = (A,A′), (A,B), and (A′,B), respectively. The β_{ij} values are practically zero for other nearest-neighbor pairs (i,j). As expected, therefore, the β_{ij} value for the dimer (A,A′) is much larger than that for any other pair.

Finally, we note that the electrical conductivity of [Au(DDDT)$_2$]^0 measured by the four-probe technique on a single crystal is about 10^{-4} Ω^{-1} cm^{-1} at room temperature.

Concluding Remarks

The crystal of [Au(DDDT)$_2$]^0 molecules exhibits a dimerlike packing motif, as in the crystal of neutral ET molecules. This is due in large part to the structural similarity of ET and [Au(DDDT)$_2$]^0 molecules. In terms of valence electrons, [Au(DDDT)$_2$]^0 and [Ni(DDDT)$_2$]$^-$ complexes are isoelectronic. Our MO calculations suggest that the metal ions of both complexes are best described by d^8 ions, and an unpaired electron in each molecule is primarily represented by the π^* orbitals of DDDT ligands with a small contribution from the metal d_{yz} orbital. In contrast to the case of (Et$_4$N)[Ni(DDDT)$_2$] and [(n-Bu)$_4$N][Ni(DDDT)$_2$], the crystal of [Au(DDDT)$_2$]^0 molecules does not give ESR signals. This is likely to be a result of strong spin-Peierls distortion, as evidenced by the dimerlike packing motif of the crystal.

[Ni(DDDT)$_2$]$^-$ molecules form layers in (Et$_4$N)[Ni(DDDT)$_2$] but stacks in [(n-Bu)$_4$N][Ni(DDDT)$_2$]. Thus, the nature of interaction between [Ni(DDDT)$_2$]$^-$ molecules can be modified by the length and shape of the alkyl group in a tetraalkylammonium ion. This observation is expected with [Ni(DDDT)$_2$]$^-$ molecules are required to pack closely around each tetraalkylammonium ion.

Acknowledgment. Work at Argonne National Laboratory was sponsored by the U.S. Department of Energy, Office of Basic Energy Sciences, Division of Materials Sciences, under Contract W-31-109-Eng-38. Research at North Carolina State University was supported in part by DOE, Office of Basic Sciences, Division of Materials Sciences, under Grant DE-FG05-86-ER45259. We express our appreciation for computing time made available by DOE on the ER-Cray computer. Work in Copenhagen was supported by SNF-Grant No. 5.21.99.38. T.L.S., from the University of Massachusetts, Boston, MA, is a Student Research Participant sponsored by the Argonne Division of Educational Programs.

Registry No. [(n-Bu)$_4$N]$^+$**1**$^-$ (M = Au), 110487-47-3; **1** (M = Au), 107240-10-8; [(n-Bu)$_4$N]$^+$**1** (M = Ni), 103123-25-7; **1**$^{2-}$ (M = Au), 107311-07-9; **1**$^+$ (M = Au), 110487-48-4; TTBED, 74962-29-1; $KAuBr_4$, 14323-32-1; [(n-Bu)$_4$N]$AuCl_4$, 17769-64-1; [(n-Bu)$_4$N]Br_3, 38932-80-8.

Supplementary Material Available: Tables of anisotropic thermal parameters for [Au(DDDT)$_2$]^0 and [(n-Bu)$_4$N][Ni(DDDT)$_2$] (2 pages); tables of observed and calculated structure factors (9 pages). Ordering information is given on any current masthead page.